Plant Science 326 (2023) 111503

Contents lists available at ScienceDirect

Plant Science

journal homepage: www.elsevier.com/locate/plantsci

Fructose-6-phosphate-2-kinase/fructose-2,6-bisphosphatase regulates energy metabolism and synthesis of storage products in developing rice endosperm

Xiaoli Chen [a,1], Yi Ji [a,1], Weiying Zhao [a], Huanying Niu [a], Xue Yang [a], Xiaokang Jiang [a], Yipeng Zhang [a], Jie Lei [a], Hang Yang [a], Rongbo Chen [a], Chuanwei Gu [a], Hongyi Xu [a], Hui Dong [a], Erchao Duan [a], Xuan Teng [a], Yunlong Wang [a], Yuanyan Zhang [a], Wenwei Zhang [a], Yihua Wang [a,*], Jianmin Wan [a,b,*]

[a] State Key Laboratory of Crop Genetics and Germplasm Enhancement, Jiangsu Plant Gene Engineering Research Center, Nanjing Agricultural University, Nanjing 210095, PR China

[b] National Key Facility for Crop Gene Resources and Genetic Improvement, Institute of Crop Sciences, Chinese Academy of Agricultural Sciences, Beijing 100081, PR China

ARTICLE INFO

Keywords:
Fru-2
6-P_2
Glycolysis
Energy metabolism
Starch synthesis
Oryza sativa

ABSTRACT

Starch accounts for about 80–85 % of the dry weight of grains and determines yield by impact on grain weight. And, the content and composition of starch also determine appearance, eating, cooking and nutritional quality of rice. By coordinating crucial reactions of the primary carbohydrate metabolism in all eukaryotes, fructose-2,6-bisphosphate (Fru-2,6-P_2) is a traffic signal in metabolism. However, the metabolic regulation of starch in plant sink tissues by Fru-2,6-P_2 remains unclear. Here we isolated rice mutant *floury endosperm23* (*flo23*) which has opaque endosperm and anomalous compound starch grains (SGs). *flo23* mutant grains had reduced contents of starch, lipids and proteins. Map-based cloning and genetic complementation experiments showed that *FLO23* encodes a cytoplasmic Fructose-6-phosphate-2-kinase/Fructose-2,6-bisphosphatase (F2KP). Mutation of OsF2KP2 decreased Fru-2,6-P_2 content in endosperm cells, leading to drastically reduced phosphoenolpyruvate (PEP) and pyruvate contents and disordered glycolysis and energy metabolism. The results imply that OsF2KP2 participates in the glycolytic pathway by providing precursors and energy for synthesis of grain storage compounds.

1. Introduction

Starch, accounting for 90 % grain weight in the milled rice, is the predominant carbohydrate source for human and industry, except for providing energy for seed germination and early seedling growth. Starch biosynthesis is a sophisticated but orderly process that coordinately utilizes critical enzymes and regulatory factor, which content and composition largely determine the yield and quality of rice. In rice, the majority of CO_2 is fixed in the leaves and then is transported into sink tissue such as root, flower and seed taking sucrose as the main sugar. In sink tissue, sucrose is cleaved into glucose, fruticose and UDP-glucose (UDP-G). Glucose is phosphorylated to glucose-6-phosphate (G6P) by hexokinase (HXK) and then transferred into ADP-glucose (ADP-Glc) catalyzed by Adenosine 5′-diphosphate (ADP) pyrophosphorylase (AGPase) to initiate starch synthesis. After that, the glucan chains of starch are elongated and modified by starch synthases (SSs), starch branching enzymes (SBEs) and starch debranching enzymes (DBEs) and so on. Mutations in these key enzymes cause abnormal endosperm phenotypes, such as *waxy*, *sugary1/isa1*, *shrunken*, *flo5*, and *sbe1* (Ryoo et al., 2007; Fujita et al., 2011; Tang et al., 2016; Toyosawa et al., 2016; Satoh et al., 2003; Kawagoe et al., 2005). In addition to enzymes directly involved in synthesizing starch other factors indirectly regulating starch synthesis and grain quality have been reported. Various rice mutants with opaque endosperm were named floury, such as *flo2*, *flo6*, *fse*, *flo11*, and *flo15* (She et al., 2010; Suzuki et al., 2020; Peng et al., 2014; Long et al., 2018; Zhu et al., 2018; You et al., 2019; Tabassum et al., 2020).

* Correspondence to: State Key Laboratory of Crop Genetics and Germplasm Enhancement, Nanjing Agricultural University, Nanjing 210095, PR China.
E-mail addresses: yihuawang@njau.edu.cn (Y. Wang), wanjm@njau.edu.cn, wanjianmin@caas.cn (J. Wan).

[1] These authors contributed equally to this work.

https://doi.org/10.1016/j.plantsci.2022.111503
Received 10 August 2022; Received in revised form 2 October 2022; Accepted 13 October 2022
Available online 19 October 2022

Other genes involved in energy metabolism also modulate starch biosynthesis by delivering intermediate products and ATP, such as *OsAlaAT1*, *OsNDUFA9*, *OsNPPR1*, *FLO10*, *FLO16*, *FLO18*, *FLO19* (Hu et al., 2018; Wu et al., 2019; Yu et al., 2021; Zhong et al., 2019; Lei et al., 2022; Hao et al., 2019; Teng et al., 2019).

Fructose-2,6-bisphosphate (Fru-2,6-P_2) plays a pivotal role primary carbohydrate metabolism in all eukaryotes. In plant source tissues, it orchestrates the photosynthetic carbon flux into biosynthesis of sucrose and starch, as previously shown to control sucrose biosynthesis in rice leaves *via* Fru-2,6-P_2 concentration during daytime (Park et al., 2007). The synthesis and degradation of Fru-2,6-P_2 is catalyzed by 6-phosphofructo-2-kinase and fructose-2,6-bisphosphatase. Their activities in plants are dependent on a single bifunctional enzyme, namely F2KP. F2KPs possess a conserved catalytic domain and a plant-specific N-terminal region. Their activities are subjected to complex allosteric regulation by primary intermediate metabolites (Nielsen et al., 2004; McCormick and Kruger, 2015). Direct regulation of Fru-2,6-P_2 on photosynthetic carbon metabolism was demonstrated through heterologous expression and antisense/RNAi suppression of *F2KP* expression (Nielsen et al., 2004; Lee et al., 2006). Fru-2,6-P_2 content in plant leaves alters photosynthetic carbohydrate partition. Half Fru-2,6-P_2 content in transgenic tobacco enhanced sucrose synthesis and suppressed starch synthesis in a similar way to Arabidopsis and other broad-leafed species (Scott et al., 2000; Szoke et al., 2007; Draborg et al., 2001; Rung et al., 2004).

Fru-2,6-P_2 enhances glycolysis by inhibiting cytosolic fructose-1,6-bisphosphatase (cFBPase, EC 3.1.3.11) and activating phosphofructokinase (PFK, EC 2.7.1.11) in non-plant organisms, nevertheless there are fundamental differences in regulatory systems in plants (Nielsen et al., 2004; Stitt, 1990a, 1990b; Nielsen and Stitt, 2001). Mutations in essential enzymes in rice gluconeogenesis and glycolysis also result in floury endosperm. Mutation in the pyrophosphate: fructose-6-phosphate 1-phosphotransferase (PFP, EC 2.7.1.90) β subunit ($PFP1_{\beta}$) impaired starch biosynthesis and disrupted the lipid and glycolytic pathways during endosperm development (Chen et al., 2020; Duan et al., 2016). The pyruvate kinase (PK) complex is the critical enzyme for production of pyruvate and ATP which generates energy for starch synthesis during grain filling; and mutation causes pleiotropic defects, including dwarfism, diminished grain weight, and poor grain quality (Zhang et al., 2012; Hu et al., 2020; Cai et al., 2018a, 2018b). Pyruvate orthophosphate dikinase (PPDK)/FLO4 is responsible for the reversible conversion of pyruvate and Pi to phosphoenolpyruvate (PEP) and inorganic pyrophosphate (PPi), providing carbon skeletons for amino acid and lipid synthesis and for manipulating the partition of ADP-Glc into starch and lipids (Wang et al., 2018, 2020a; Zhou et al., 2016). Although these results showed that glycolysis is critical for endosperm development the energy balance between glycolysis and starch synthesis in rice endosperm remained unknown.

In this study, we isolated and identified an opaque endosperm rice mutant named *flo23* with abnormal amyloplasts. The *FLO23* allele encodes a 6-phosphofructo-2-kinase/fructose-2,6-bisphosphatase bifunctional enzyme (F2KP). F6P,2-K activity is reduced in *flo23* mutant which leads to reduction of Fru-2,6-P_2 level. Our findings indicated that FLO23 affects key enzymes in the glycolytic metabolic pathway that are essential for energy and synthesis of storage compounds in endosperm cells.

2. Materials and methods

2.1. Plant materials and growth conditions

The *flo23* mutant was screened from MNU (*N*-methyl-*N*-nitrosourea)-treated *indica* variety cultivar N22. The *f41* mutant was obtained from a mutant library developed from *japonica* variety Ningjing4 following MNU treatment. An F_2 mapping population was derived from a cross between the *flo23* mutant and *indica* cultivar 93–11. All plants were grown in experimental fields at the Tuqiao and Pailou Research Stations of Nanjing Agricultural University.

2.2. Microscopy

Cross sections of the mature grains were covered with gold powder and observed with a HITACHI S-3000 N scanning electron microscope (Hitachi, Tokyo). For transmission electron microscopy (TEM) samples of approximately 1 mm thickness from the middle part of the developing endosperm were fixed, dehydrated and embedded in LR-White resin (London Resin, Berkshire, UK) as described (Zhu et al., 2021). Semi-thin (1 μm) sections were prepared and stained with 1 % iodine-potassium iodide (I_2-KI) as described previously (Wu et al., 2019), and photographed using a light microscope (Nikon ECLIPSE80i, Tokyo).

2.3. Seed metabolite analysis

Mature rice seeds were dehulled and ground into fine powder for analysis of storage products. The contents of total starch, amylose, protein, and lipids, and amylopectin chain length distribution, were determined as previously described (Han et al., 2012). Levels of soluble seed sugars (sucrose, glucose and fructose) were measured with a Waters Ultra-high Performance Liquid Chromatograph (Water, Hclass). 1 mL of 80 % ethanol was added to 50 mg of fresh ground endosperm from seeds at 9 DAF and incubated at 80 °C for 30 min, then ultrasonic extraction at 80 °C for 30 min, centrifuging at 12,000 *g* for 15 min, and collection of the supernatant. The procedure was repeated and the supernatants were combined, evaporated to dryness under vacuum at 45 °C, dissolved in ultrapure water preheated at 50 °C, and passed through a pre-activated C18 extraction cartridge prior to determination of the sugar content. PEP and pyruvate were extracted from developing seeds using perchloric acid and concentrations were determined using an NADH fluorescence assay, as previously described (Häusler et al., 2000).

2.4. Map-based cloning of the FLO19 gene

A F_2 population was obtained from crossing *flo23* mutant with cultivar 93-11. Ten individuals with floury seeds segregated from this F_2 population were used for preliminary mapping. Furthermore, 532 floury individuals were used for fine mapping. In addition, whole genome sequencing analysis was performed to genomic variation between wild type and *flo23* mutant. Bringing together the whole genomic variation and fine mapped region, we carried out the prediction of candidate genes. Primers used for gene-mapping are listed in Table S1.

2.5. Genetic complementation analysis

We cloned the *OsF2KP2* coding sequence (CDS) from N22 cDNA that was introduced into binary vector pCAMBIA1305-GFP by homologous recombination with the cauliflower mosaic virus (CaMV) 35 S promoter used to drive expression of *OsF2KP2-GFP* in the *flo23* mutant. To obtain *OsF2KP2* knockout lines, a 20-bp specific guide RNA was cloned into the CRISPR/Cas9 expression vector. These recombinant vectors were introduced into the *flo23* mutant and Nipponbare by *Agrobacterium tumefaciens*-mediated transformation. Positive transgenic lines were identified by PCR and sequencing.

2.6. Multiple sequence alignment and protein tertiary structure prediction

OsF2KP2 homologous protein sequences were blasted and downloaded from NCBI. Multiple amino acid sequence alignments were performed with ESPript 3.0 website (https://espript.ibcp.fr). The SWISS-MODEL was used for protein tertiary structure prediction (https://swissmodel.expasy.org/).

2.7. GUS staining

The vector containing CDS of *β-glucuronidase* (*GUS*) driven by the *OsF2KP2* promoter (approximately 2000 bp upstream of ATG) was constructed and introduced into Nipponbare calli. T_2 generation lines were planted after PCR detection of 5 independent positive plants. The positive transgenic plants and wild type were stained as described (Teng et al., 2019). Images of various tissues were obtained with a stereoscope (Leica Application Suite 3.3, Germany).

2.8. Subcellular localization

OsF2KP2 and *OsF2KP1* CDS sequences without stop codons were inserted into the pAN580 vector driven by the CaMV 35 S promoter. Plasmids were separately transformed into rice protoplasts as previously described (Chen et al., 2006). These fragments were cloned into binary vector pCAMBIA1305-GFP and then transformed into Agrobacterium strain *EHA105*. *OsF2KP2-GFP* was introduced into the *flo23* mutant and observations were made on root tip cells of positive transgenic seedlings. *OsF2KP1-GFP* was expressed in tobacco leaf epidermal cells and fluorescent GFP signals were observed using a Leica TCS SP8 laser-scanning confocal microscope.

2.9. RNA extraction and real-time RT-PCR analysis

Total RNAs were extracted from various plant tissues using an RNAprep Pure Plant Kit (TIANGEN Biotech, Beijing). Approximately 1 μg of total RNA was used for first-strand synthesis in a 20 μL volume with a HiScript® II 1st Strand cDNA Synthesis Kit (Vazyme, Nanjing). Real-time PCR was applied using Bio-Rad T100TM real-time PCR system (California) with the Genious 2 × SYBR Green Fast qPCR mix (Abclonal, Cat# RM21204). The rice *Ubiquitin* gene was used as an internal control. Primers are listed in Table S1.

2.10. SDS-PAGE and immunoblot analysis

Total protein extraction and immunoblotting were performed following the method described by Wang et al. (2010). Polyclonal antibodies were used as previously described (Cai et al., 2018b). Anti--EF-1α antibodies raised in rabbits were used as a loading control (Abclonal, Wuhan).

2.11. Yeast two-hybrid (Y2H) assay

The CDSs of *OsF2KPs* were recombined into the pGADT7 and pGBKT7 vectors. Yeast transformation of recombinant resultant plasmids and screening processes were performed following the manufacturer's instructions. The different resulting recombinant plasmids involving *OsF2KPs* were transformed into yeast stain AH109. Yeast cells were grown in selective medium at 30 °C for 3–5 days.

2.12. Bimolecular fluorescent complementation (BiFC) assays

Full-length *OsF2KP2* and *OsF2KP1* cDNA for BiFC assays were cloned into p2YC and p2YN, respectively. The constructed vectors were transformed into *A. tumefaciens* strain *EHA105*; different combinations were transiently expressed in tobacco epidermal cells and fluorescent signals were observed after incubation for 48–60 h using a confocal microscope.

2.13. Co-IP assays

The CDSs of *OsF2KP1* and *OsF2KP2* without stop codons were cloned into pCAMBIA1305-GFP vectors, and *OsF2KP2* was inserted into pCAMBIA1300–221-Flag by homologous recombination. The constructs were co-transformed into *N. benthamiana* for transient expression. Total protein was extracted with NB1 buffer (50 mM Tris-MES, pH 7.4, 0.5 M sucrose, 1 mM $MgCl_2$, 5 mM DTT, 10 mM EDTA, 0.1 % [v/v] Nonidet P-40 and Complete™ Protease Inhibitor Cocktail (50 mL extraction buffer per tablet)). Extracted total protein lysate were incubated and with Flag-beads for 2 h at 4 °C, and washed the Flag-beads five times with extraction buffer after incubation. The FLAG-beads were boiled with 1X protein loading buffer for 5 min, and perform immunization as previously described (Lei et al., 2022).

2.14. Recombinant protein production

The *OsF2KP2* and *cFBP* coding regions were inserted into the pGEX-4 T-2 vector to express fusion proteins with Glutathione S-transferase (GST) in *E. coli* strain BL21 (DE3). Firstly, positive clones were cultured in LB liquid medium at 37 °C and 220 rpm until the OD_{600} reached 0.5; 0.1 mM IPTG was added and the reaction induce at 16 °C, 120 rpm for 16 h. Fusion proteins were purified according to the manufacturer's instructions (Genscript, Cat# L00206). Purified proteins were quantified with a Bradford Assay Kit (Thermo Fisher Scientific, Cat# 23236).

2.15. Extraction and assay of Fru-2,6-P_2

Fresh endosperm was extracted in 20 vol. of ice-cold 50 mM KOH. Extracts were incubated at 80 ℃ for 5 min, cooled on ice, incubated with activated carbon (10 mg/mL), and centrifuged at 13,000 *g* for 5 min. The content of Fru-2,6-P_2 in the supernatant was analyzed by a coupled enzymatic assay based on inhibition of cFBP. The 200 μL reaction mixture contained Hepes-NaOH pH7.5, 100 mM; Fru-1,6-P_2, 5 mM; $MgCl_2$, 5 mM; EDTA, 0.5 mM; $NADP^+$, 0.5 mM; 1 U phosphoglucoisomerase, 2 U glucose-6-phosphate dehydrogenase, 10 μg recombinant cFPB, and 5 μL of supernatant. The reaction was traced by measuring absorption at 340 nm every minute for 10 min at 25 ℃. To eliminate endogenous Fru-2,6-P_2 the supernatant was hydrolyzed with perchloric acid and neutralized with NaOH, and gradient concentrations of Fru-2,6-P_2 were added as an internal standard.

2.16. Enzymatic activity assays

F6P,2-K activities were assayed using the above purified recombinant protein. The reaction buffer including Hepes-NaOH pH7.5, 100 mM; Fru-6-P, 5 mM; $MgCl_2$, 5 mM; EDTA, 0.5 mM; $NADP^+$, 0.5 mM; 1 U phosphoglucoisomerase, and 2 U glucose-6-phosphate dehydrogenase. The reaction was initiated by adding recombinant proteins to the reaction buffer. Enzyme activity was calculated as a decrease in Fru-6-P concentration. Developing endosperm at 9 DAF were homogenized in liquid nitrogen, extracted with Hepes-buffer (Hepes-NaOH pH7.5, 50 mM; $MgCl_2$, 2 mM; *β*-mercaptoethanol, 50 mM; glycerol, 12.5 % [v/v]), and centrifuged at 16,000 *g* for 10 min at 4 °C. The supernatant was used as a crude enzyme solution for enzyme assays. PFP activity was measured by determining the formation of NAD^+ in the glycolytic direction according to a previous study (van der Merwe et al., 2010). The cFBPase assay was measurement of increasing NADpHconcentration from the start of the enzymatic reaction, as previously described (Ohashi et al., 2018). AGPase activity was assayed following the method described by Teng et al (Teng et al., 2019).

2.17. Pyrophosphate (PPi) determination

About 100 mg of endosperm at 9 DAF was ground into powder in liquid nitrogen, and 1 mL of 16 % (v/v) trichloroacetic acid/diethylether solution (pre-cooled on dry ice in advance) was added and well mixed. After standing on dry ice for 15 min 400 μL of a 16 % (v/v) aqueous solution of trichloroacetic acid (containing 5 mM of EGTA) was added and shaken at 4 ℃ for 3 h to completely denature the pyrophosphatase. After centrifuging at 4 ℃ for 5 min, the lower aqueous phase was removed by syringe, the upper aqueous phase was retained. The water phase was washed 3 times by shaking with 800 μL of saturated aqueous

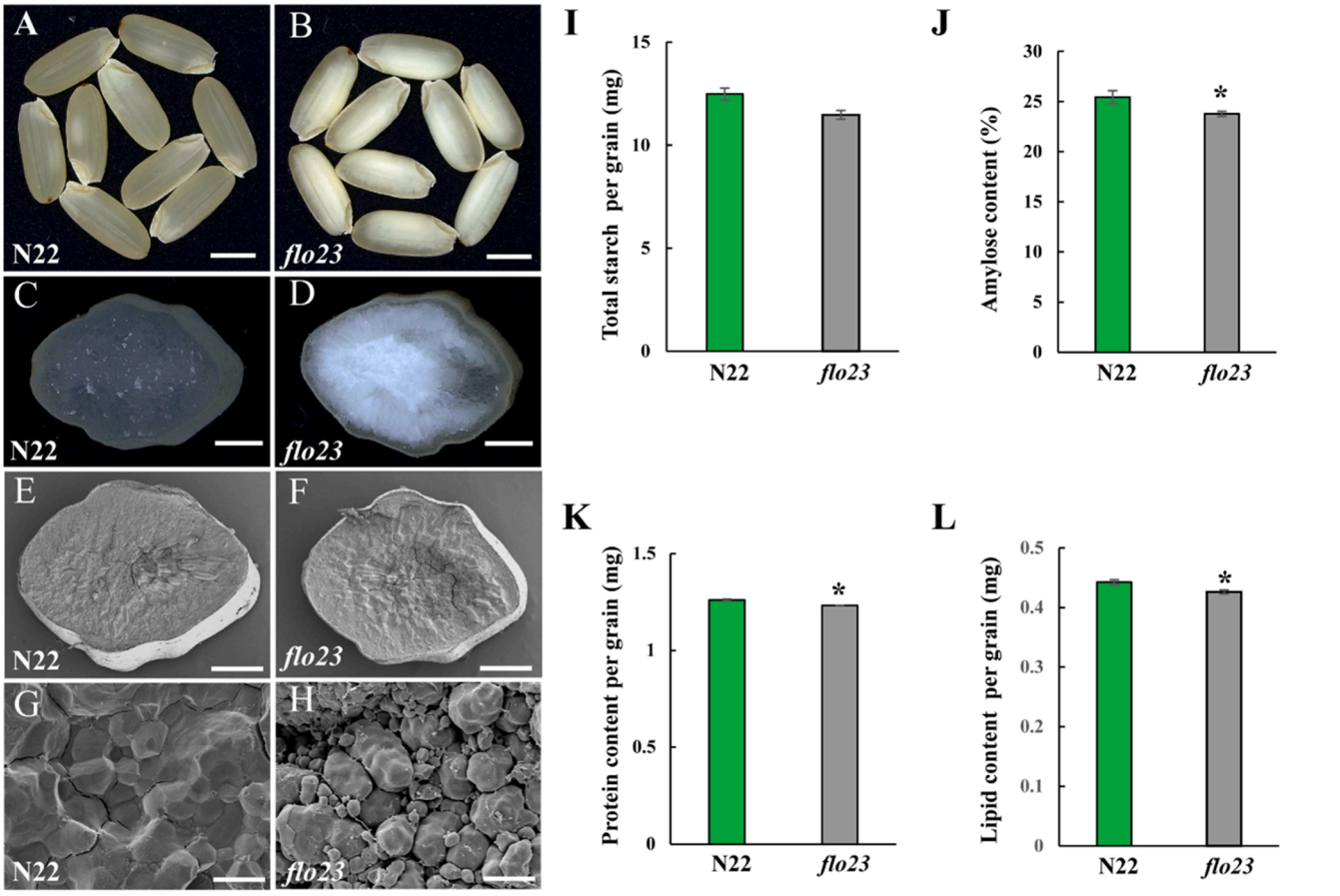

Fig. 1. Phenotypic characterization of the *flo23* mutant. (A, B) Mature grains from wild-type N22 (A) and *flo23* mutant (B). Bars, 5 mm. (C, D) Transverse sections of mature seeds of WT (C) and the *flo23* mutant (D). Bars, 1 mm. (E-F) Scanning electron microscope images of transverse sections of mature seeds from N22 (E, G) and *flo23* mutant (F, H). Bars, 0.5 mm (E, F), 20 μm (G, H). (I-L) Total starch (I), amylose (J), protein (K), and lipid (L) contents in brown rice from wild-type N22 and *flo23* mutant. Values are means ± SD, n = 3, Student's *t*-tests (* $P < 0.05$, ** $P < 0.01$).

ether solution. The aqueous phase was neutralized with 5 M KOH /1 M triethanolamine solution, and a small amount of acid-treated activated carbon was added to remove interfering compounds prior to PPi determination. Ninety μL of double-distilled water, 40 μL of 2.5 % (w/v) ammonium molybdate dissolved in 2.5 M sulfuric acid, and 10 μL of 1 M *β*-mercaptoethanol were sequentially added to a 10 μL sample. Absorbance at 580 nm was determined after standing at room temperature for 25 min.

2.18. RNA-seq analysis

Total RNA was extracted from wild type and *flo23* mutant endosperm at 9 DAF in three replications. Construction and sequencing of the cDNA library were performed with the BGISEQ-500 platform (BGI, Wuhan). The reference IRGSP-1.0 genome was used to compare clean reads obtained by filtering the sequence data. Data were analyzed on the Dr. Tom system from BGI (Table S2). PPI networks of up-regulated genes were generated by STRING (https://cn.string-db.org/) and constructed by Cytoscape 3.8.2 (https://cytoscape.org/).

2.19. Targeted metabolomic analysis

Ultra-performance liquid chromatography-tandem mass spectrometry (UPLC-MS/MS) was used to detect 30 key metabolites involved in energy metabolism at Shanghai Bioprofile (http://www.bioprofile.cn). Rice endosperm samples, each of 100 mg, were ground in liquid nitrogen and 1 mL of pre-cooled methanol/acetonitrile/water (2:2:1, v/v/v) was added to each sample. After vortexing, the mixtures were sonicated in an ice bath for 60 min and incubated at − 20 °C for 1 h to precipitate the protein. The supernatant was centrifuged at 14,000 *g* for 20 min at 4 °C and dried under vacuum. For mass spectrometry, 100 μL of acetonitrile-water solution (1:1, v/v) was added to reconstitute the sample, which was then centrifuged at 14,000 *g* at 4 °C for 15 min, and the supernatant was used for analysis. Analysis was performed using a Nexera LC-30 CE UHPLC system (Shimadzu, Japan) with an ACQUITY UPLC BEH Amide column (1.7 mm, 2.1 3 100 mm; Waters) and an QTRAP 5500 mass spectrometer (AB SCIEX).

3. Results

3.1. Phenotypic characterization of the flo23 mutant

The *flo23* mutant was isolated from an MNU (*N*-methyl-*N*-nitrosourea)-mutagenised library of rice variety aus Nagina-22 (also know as N22). Compared with wildtype, *flo23* mutant showed opaque or floury endosperm without other agronomical traits changes (Fig. 1A-D, Fig. S1A, B, E). Normally, floury endosperm is associated with changes in strach granuals (SGs) accumulation and contents of grain storage components. The SGs of the mature endosperm were arranged very densely and regular in wild type, while loosely packed, irregularly scattered spherical starch granules with large spaces in the *flo23* mutant *via* scaning electron microscopy of cross-sections (Fig. 1E-H). After fertilization, the grain filling rate of *flo23* mutant plants was slightly slower (Fig. S2A), ultimately resulting in a signifcantly reduced 1000-grain weight compared with wild type (Fig. S2B).

Compared with the wild type, analysis of the physicochemical

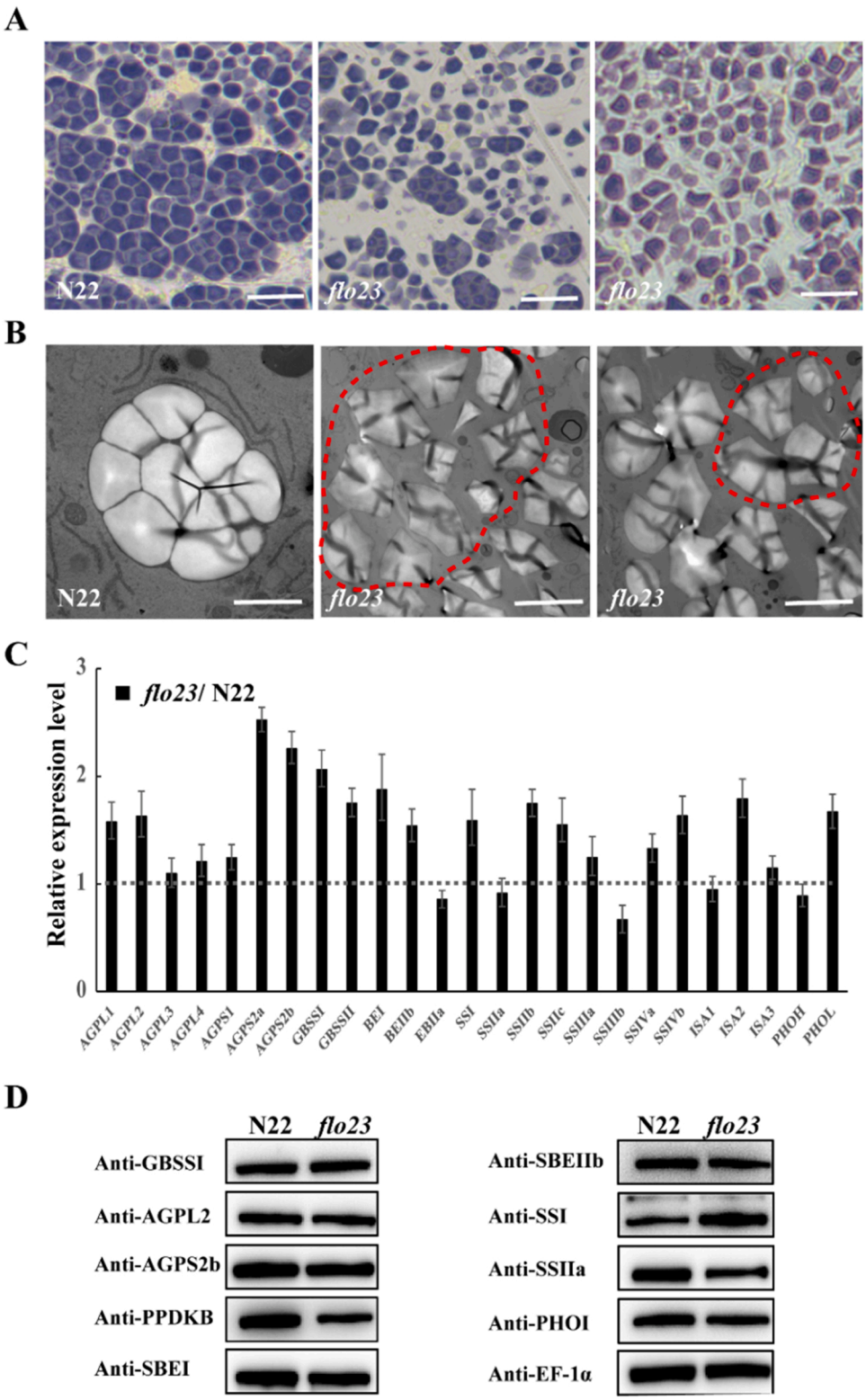

Fig. 2. Cytology, starch biosynthsis related gene expression and immunoblot analyses of developing endosperm at 9 DAF. (A) Iodine-staining of the semi-thin sections of N22 and *flo23* mutant endosperm. Bars, 5 μm. (B) Transmission electron microscopy of endosperm in N22 and the *flo23* mutant. Fragmented starch granules are encircled by dotted red lines. Bars, 2 μm. (C) Expression levels of starch synthesis-related genes. The data are ratios of expression in the *flo23* mutant to the wild type. Values are means ± SD, n = 3. (D) Immunoblot analyses of starch synthesis-related enzymes in wild-type and *flo23* mutant endosperm with polyclonal antibodies raised against GBSSI, AGPL2, AGPS2b, cytosolic PPDKB, SBEI, SBEIIb, SSI, SSIIa and PHOI. EF-1α was used as the loading control.

properties showed that total starch, proteins and lipid were slightly decreased, and amylose contents also decreased in the *flo23* mutant (Fig. 1I-L). Soluble sugar contents in the *flo23* mutant was increased slightly (Fig. S2C). Measement of the amylopectin chain length distribution showed that the degree of polymerization of 5–11 starch chains was decreased whereas the polymerization other components was increased (Fig. S2D). The overall evidence indicated that starch biosynthesis was compromised and physicochemical characteristics were altered in *flo23* mutant.

3.2. Abnormal starch grain development in flo23 mutant endosperm

Numerous compound starch grains (SGs) are formed and filled during endosperm development. Observations of semi-thin sections of developing endosperm at 9 days after fertilization (DAF), compound SGs with sharp-edged polyhedral structures filling the entire endosperm cells

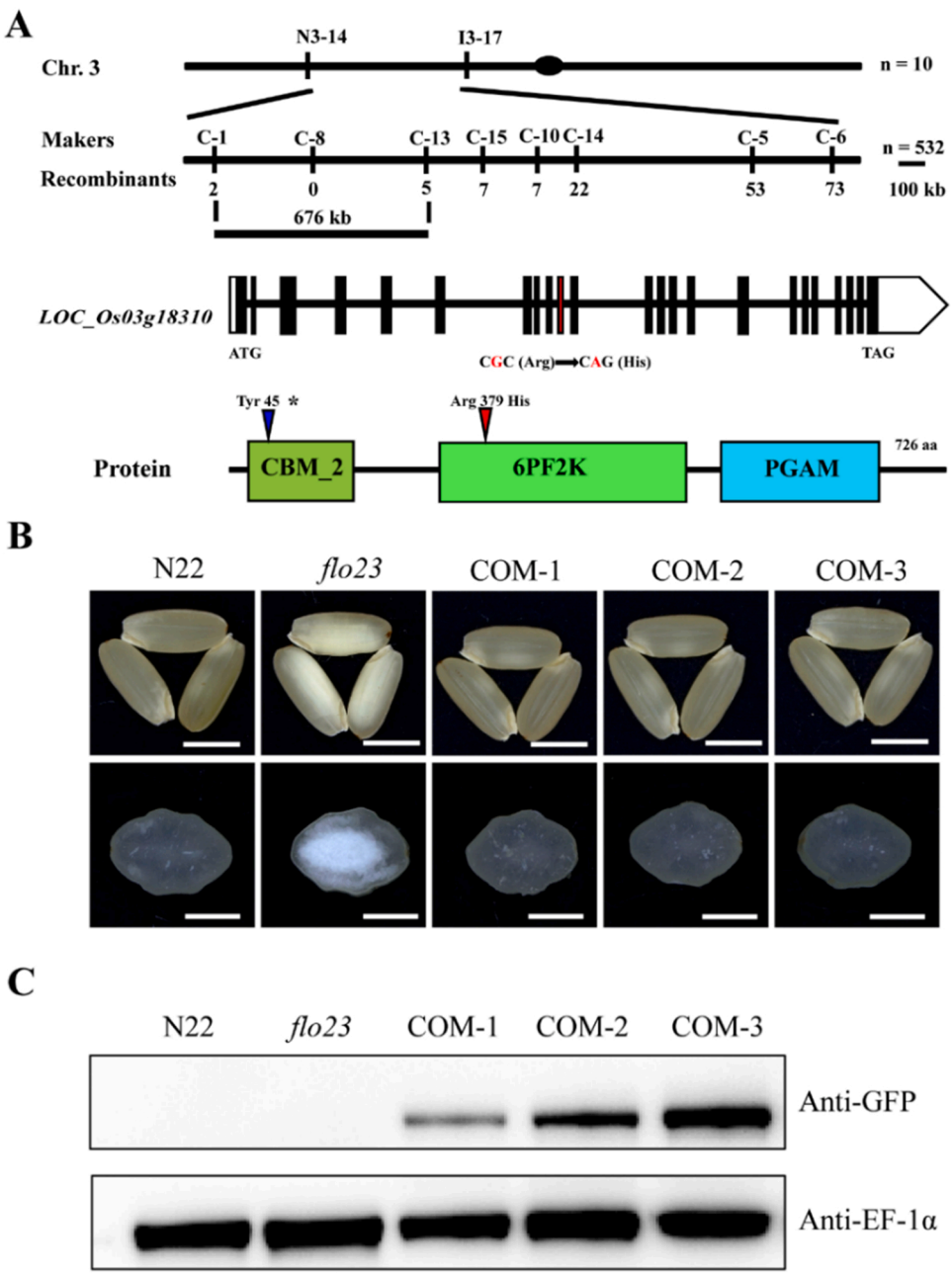

Fig. 3. Map-based cloning of *FLO23*. (A) The *FLO23* locus was fine-mapped to a 676 kb interval between markers C-1 and. C-13 on chromosome 3. The candidate *FLO23* gene was identified by whole genome resequencing. G to A substitution in the 10th exon caused a change of amino acid 379 from Arg to His (red arrowhead). G to A mutation in mutant *f41* caused a premature stop codon (blue arrowhead). (B) Genetic complementation of *flo23* restored translucent seed appearance. COM-1, COM-2 and COM-3 are three independent positive transgenic lines transformed with *35 S::FLO23-GFP* in the *flo23* mutant. Bars, 3 mm (upper panel) and 1 mm (lower panel). (C) Immunoblot analysis of total seed proteins in developing seeds of the wild type, *flo23* mutant and three complemented transgenic lines with GFP monoclonal antibody. EF-1α was used as the loading control.

in the wild type (Fig. 2 A). However, more fragmented and lightly purple iodine-stained stained SGs in the *flo23* mutant were observed by (Fig. 2A). Transmission electron microscopy confirmed those results that SGs from *flo23* mutant were fragmented (Fig. 2B). These obervations revealed that normal starch grains were rarely formed in the *flo23* mutant. Normally, abnormal starch grain formation was accompanied by impaired expression levels of genes associated with starch synthesis, so we performed real-time quantitative PCR (RT-qPCR) analysis to examine the expression of them. The results showed most of genes associated with starch synthesis were up-regulated in the *flo23* mutant compared to the wild type (Fig. 2 C). Furtheremore, we analyze the abundance of proteins involved in starch synthesis in endosperm at 9 DAF by immunoblotting, and the results showed the up-regulated gene expression did not impact on the level of starch synthesis proteins wildly like GBSSI, AGPL2, AGPS2b and so on. But, the abundance of SSIIa was decreased while SSI increased in *flo23* mutant which is consistent to the gene expression level (Fig. 2 C and 2D). In addition, OsPPDKB/FLO4, encoding pyruvate orthophosphate dikinase, is associated with floury endosperm (Wang et al., 2020b). We found that the abundanc of OsPPDKB was significantly reduced in the *flo23* mutant too (Fig. 2D). Taking together, the defective compound starch grain in *flo23* mutant was possibly caused by deficiency in starch biosynthesis during endosperm development.

3.3. Map-based cloning of FLO23

Using the F_2 polulation from *flo23* mutant crossed with wild type, about a quarter of floury endosperm grains were indetified (373 of 1063, $\chi^2_{3:1} = 0.679 < \chi^2_{0.05,1} = 3.84$), indicating that the mutation was caused by a single locus. To isolate the candidate gene(s) in the *flo23* mutant, a F_2 mapping population was constructed by *flo23* mutant hybrided with 93–11. Firstly, 10 individuals, showing floury endosperm, were used to primary mapping. *flo23* locus was localized in a 6.3 Mb physical interval flanked by SSR marker *N3–14* and InDel marker *I3–17* on the long arm of

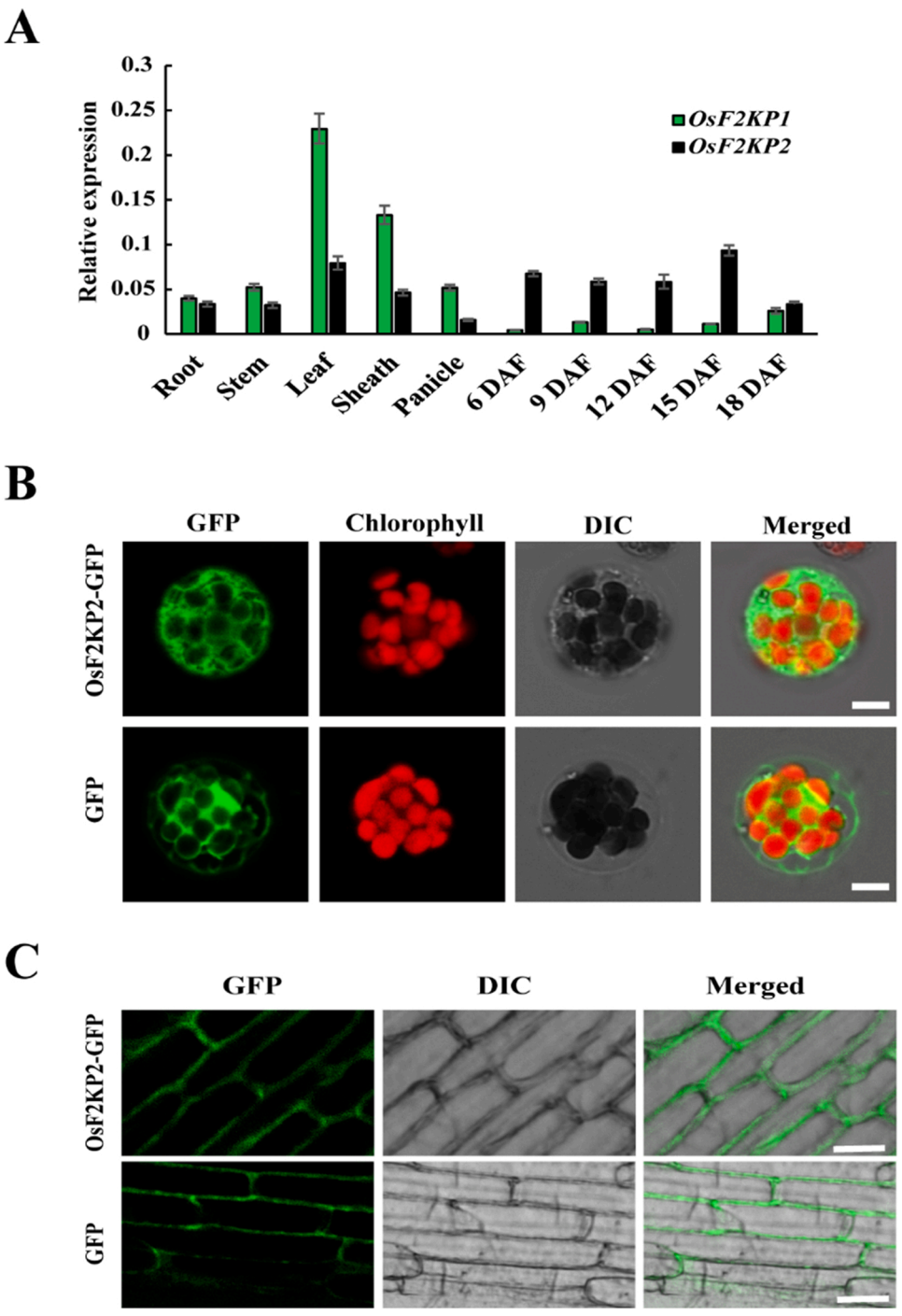

Fig. 4. Expression pattern and subcellular localization of OsF2KP2. (A) RT-qPCR analysis of relative *OsF2KP2* expression levels in various plant tissues and developing endosperm at 6–18 DAF. Rice *Ubiquitin* was used as the internal control. Values are means ± SD, n = 3. (B) Subcellular localization of OsF2KP2 in rice protoplasts. Free GFP protein was localized to the cytosol and nucleus. Bars, 10 μm. (C) GFP fluorescence in root tip cells of *flo23* mutant plants transformed with *35 S::OsF2KP2-GFP* (upper panel) and Nip transformed with *35 S:: GFP* (lowed panel). Bars, 25 μm.

chromosome 3. And then, this interval was narrowed to 676 kb by using 532 mutant individuals from mapping population. We also compared the whole genome varication by whole genome resequencing of the wild type and *flo23* mutant. Taking our fine-mapping results together, a high confidence SNP and in the coding region of *LOC_Os03g18310* was identified. A G to A transition at position 1136 of *LOC_Os03g18310* CDS leads a amino acid substitution (Argine to Histone) (Fig. 3 A). Protein sequence alignment and tertiary structure prediction indicated that Arg379 was a highly conserved active site (Figs. S3, S4). In addition, we isolated another floury mutant *f41* which harbored a G-to-A substitution at position 134, resulting in a premature stop codon (Fig. S1C, D, F).

To confirm the candicate gene, a vector containing the *LOC_Os03g18310* coding sequence fused to green fluorescent protein (GFP), driven by the cauliflower mosaic virus (CaMV) 35 S promoter was constructed and transformed into the *flo23* mutant. Mature seeds of positive transgenic lines had a restored transparent endosperm (Fig. 3B). Immunoblotting experiments also confirmed increased FLO23-GFP protein levels in the transgenic lines (Fig. 3 C). In addition, CRISPR/Cas9 knockout lines of *LOC_Os03g18310* displayed floury-white endosperm phenocopied to *flo23* mutant (Fig. S5). All of our results clearly demonstrated that mutations in *LOC_Os03g18310* were responsible for the *flo23* mutant phenotype.

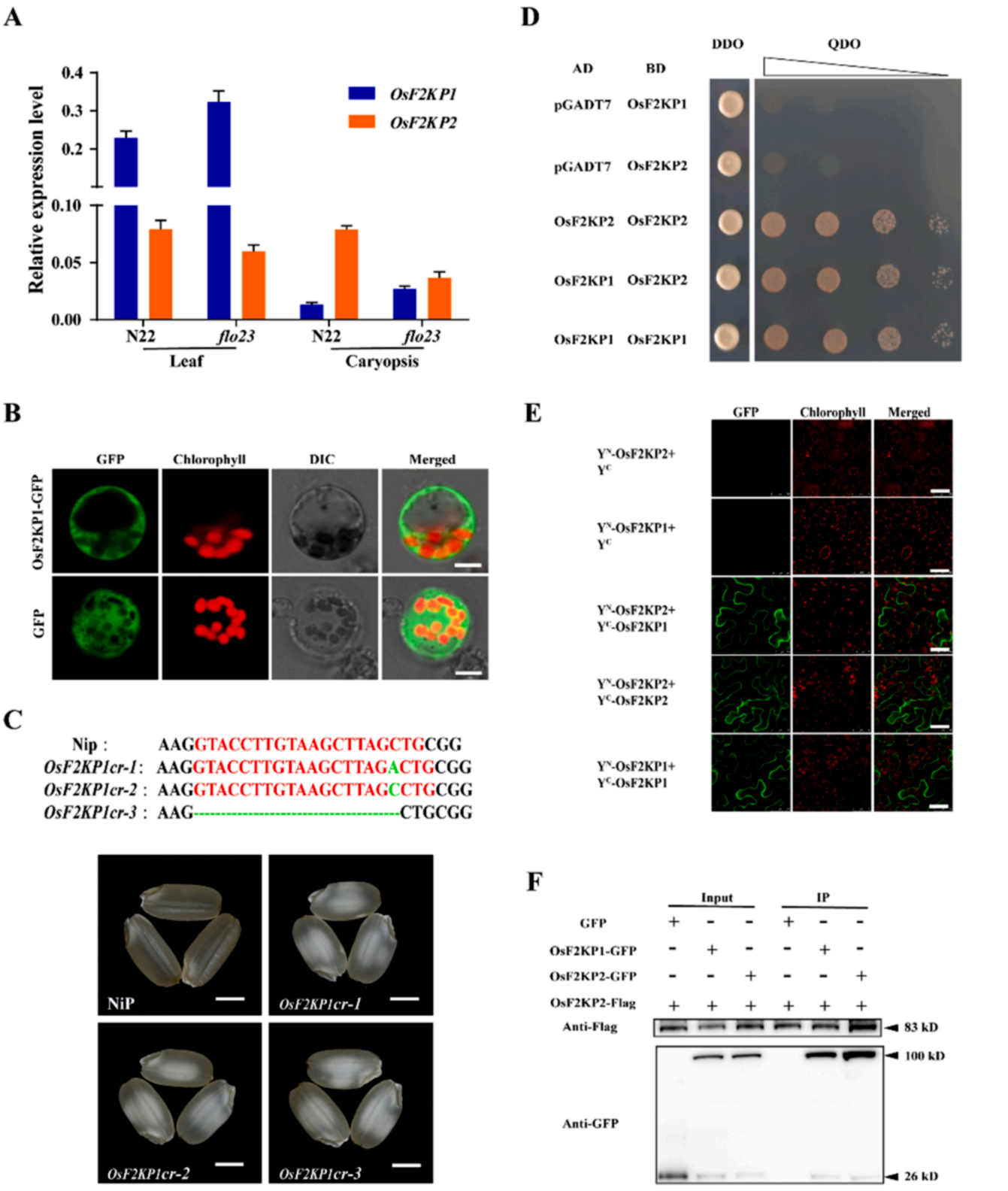

Fig. 5. OsF2KP protein assembles as multimers. (A) RT-qPCR analysis of the expression levels of *OsF2KP1* and *OsF2KP2* in the wild type and *flo23* mutant. Rice *Ubiquitin* was used as an internal control. Values are means ± SD, n = 3. (B) Subcellular localization of OsF2KP1 in rice protoplasts. Free GFP was used as the control. Bars, 10 μm. (C) Mature seeds of wild type and *OsF2KP1* knockout lines. Bars, 2 mm. Nip, Nipponbare. *OsF2KP1cr-1*, *OsF2KP1cr-2* and *OsF2KP1cr-3* are representative CRISPR/Cas9 knockout lines. (D) Interactions between OsF2KPs examined by yeast two-hybrid (Y2H) assays. DDO, control medium (SD/-Trp-Leu); QDO, selective medium (SD/-Trp-Leu-His-Ade). (E) BiFC assays showing interactions of OsF2KPs. Bars, 50 μm. (F) Interaction of OsF2KP1 and OsF2KP2 in Co-IP assays. Flag-beads were used to immune-precipitate the OsF2KP1-GFP and OsF2KP2-GFP proteins. Gel blots were probed with anti-GFP and anti-Flag antibodies, respectively.

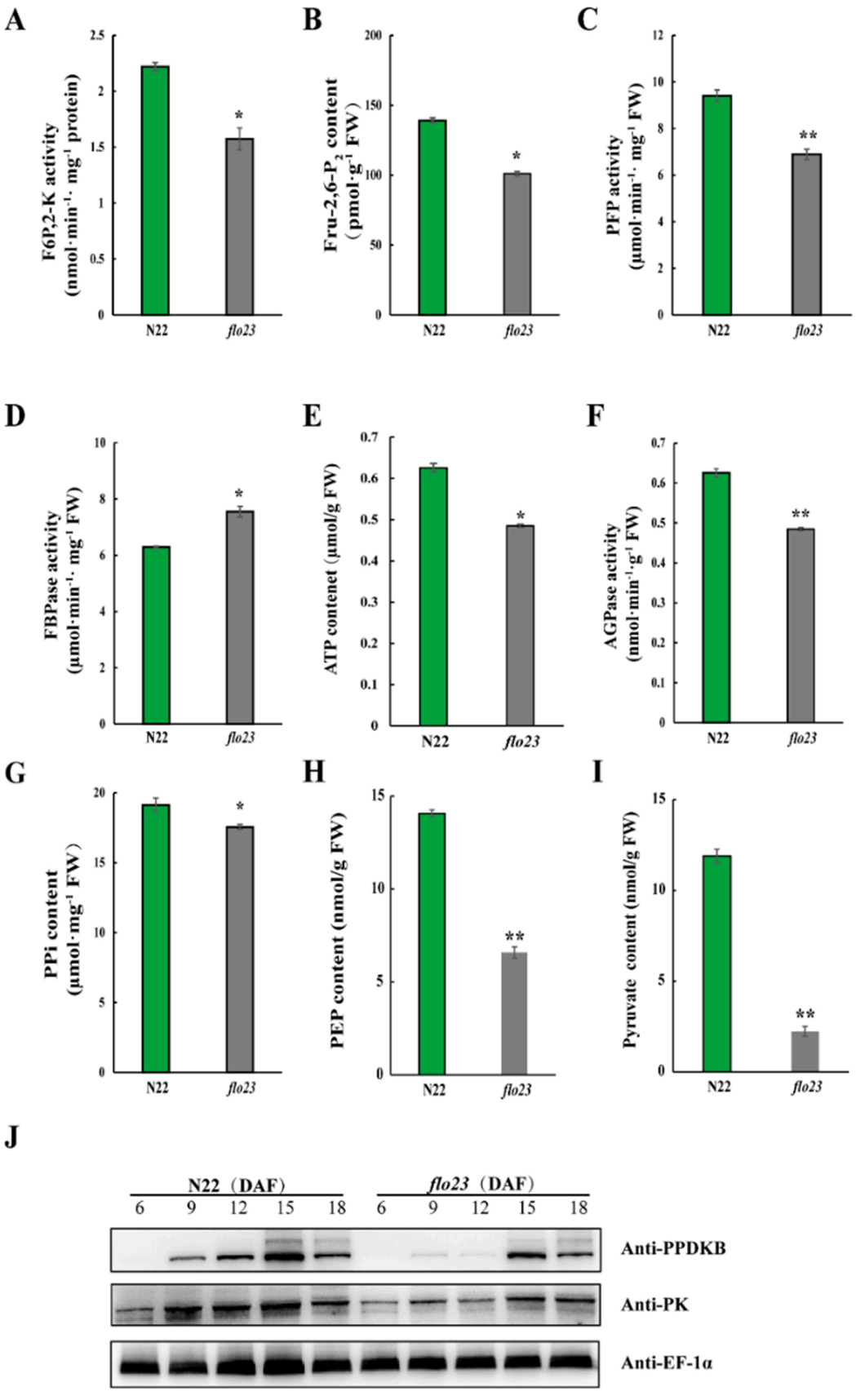

(caption on next page)

Fig. 6. OsF2KP2 affects PPi-dependent metabolic pathways in rice endosperm. (A) Activities of *in vitro*-purified F6P,2-K from the wild type and *flo23* mutant GST-OsF2KP2. Values are means ± SD, n = 3. (Student's *t*-test, * $P < 0.05$). (B) Determination of Fru-2,6-P_2 content in endosperm at 9 DAF in the wild type and *flo23* mutant. Values are means ± SD, n = 3. (Student's *t*-test, * $P < 0.05$). (C, D) Enzyme activities assays of PFP (C) and FBPase (D) in wild type and *flo23* mutant endosperms at 9 DAF. Values are means ± SD, n = 3. (Student's *t*-test, * $P < 0.05$, ** $P < 0.01$). (E) ATP content in developing endosperm at 9 DAF in the wildtype and *flo23* mutant. Values are means ± SD, n = 3. (Student's *t*-test, * $P < 0.05$). (F, G) AGPase activity (E) and PPi content (F) developing endosperm of the wild type and *flo23* mutant at 9 DAF. Values are means ± SD, n = 3. (Student's *t*-test, * $P < 0.05$, ** $P < 0.01$). (H, I) PEP (H) and pyruvate (I) contents in developing endosperm at 9 DAF from the wild type and *flo23* mutant. Values are means ± SD, n = 3. (Student's *t*-test, * $P < 0.05$; ** $P < 0.01$). (J) Changes in PK and PPDKB protein levels during endosperm development.

3.4. *FLO23 encodes a cytoplasm-localized bifunctional enzyme, fructose-6-phosphate-2-kinase/fructose-2, 6-bisphosphatase*

FLO23 was predicted to encode a bifunctional enzyme fructose-6-phosphate-2-kinase/fructose-2,6-bisphosphatase (F2KP) with 726 amino acids. It contains a plant-specific N-terminal region, a FPK domain in the center, and a FBP domain at the C-terminus (Fig. 3 A). In *japonica* rice cultivar, two genes was predict to encode F2KP, *OsF2KP1* (*LOC_Os05g07130*) and *OsF2KP2* (*LOC_Os03g18310*) (Park et al., 2007). Thus *FLO23* was renamed as *OsF2KP2*. Protein sequence alignment proved that F2KPs were widespread across species, and that the catalytic region was highly conserved in the two OsF2KPs which shared 68 % identity at the amino acid level (Fig. S3, Fig. S6). We analyzed the expression pattern of *OsF2KP1* and *OsF2KP2* by RT-qPCR in different tissues. The results showed that *OsF2KP1* mainly expressed in vegetative tissue, such as leaf and sheath. But *OsF2KP2* was expressed in most organs and showed higher expression level in grain-filling stage during the development of caryopsis, *OsF2KP2* (Fig. 4 A). GUS staining in transgenic plants with the *OsF2KP2* promoter driving the *β-glucuronidase* (GUS) coding sequence also confirmed that *OsF2KP2* was ubiquitously expressed in rice (Fig. S7). *OsF2KP2* was predicted to encode a cytosolic protein (http://www.cbs.dtu.dk/services/TargetP/), we generated an *OsF2KP2-GFP* fusion construct driven by 35 S promoter to infect rice protoplasts. Similar to free GFP the fusion protein was evenly distributed in the cytosol (Fig. 4B). GFP fluorescence in the cytosol was confirmed in root tip cells of transgenic seedlings carrying *OsF2KP2-GFP* (Fig. 4 C). Therefore, OsF2KP2 is a cytosol-localized protein.

3.5. *OsF2KP2 functions through homo and heterocomplexes*

OsF2KP1 and OsF2KP2 showed 68 % protein sequence similarity, we also analyze the function *OsF2KP1*. Firstly, we compared the expression of *OsF2KP1* in the *flo23* mutant and wild type, we found that the expression of *OsF2KP1* was slightly elevated both in leaves and caryopsis (Fig. 5 A). Secondly, OsF2KP1 also cytosolically localized and CRISPR/Cas9 knockout lines displayed white-core endosperm (Fig. 5B and C). We further analyzed the contents of storage products in the *OsF2KP1cr* mature caryopsis, but there were no significant difference (Fig. S8). The weak endosperm phenotype in *OsF2KP1cr* maybe due to different expression pattern, and up-regulated *OsF2KP1* in *flo23* mutant maybe called to compensate for the function loss in *OsF2KP2*.

It was previously reported that F2KP functions through a homotetramer in spinach (Markham and Kruger, 2002). We wondered whether the OsF2KP1 and OsF2KP2 could interact each other to form the complex in rice. The results from yeast two-hybrid assays (Y2H) indicated that OsF2KP2 interacted with itself and OsF2KP1 (Fig. 5D). Bimolecular fluorescence complementation (BiFC) experiments and co-immunoprecipitation (Co-IP) assays in the leaf of *N. benthamiana* further confirmed this interaction (Fig. 5E and F). These results suggested that OsF2KPs function in homo or heterocomplex in rice.

3.6. *OsF2KP2 affects PPi-dependent metabolic pathways in rice endosperm*

F2KP functions in catalyzing reversible conversion between fructose 6-phosphate and Fru-2,6-P_2 (Stitt, 1990a). To investigate whether the mutation affected OsF2KP2 enzymatic activity, we expressed GST-tagged recombinant proteins in *E. coli*. F6P,2-K activity of purified mutant OsF2KP2 protein was significantly decreased (Fig. 6 A). We further detected the content of Fru-2,6-P_2 *in vivo* and found the significant reduction of Fru-2,6-P_2 in *flo23* mutant endosperm at 9 DAF (Fig. 6B). The previous studies showed that Fru-2,6-P_2 activates PFPase and inhibits cFBPase (Nielsen et al., 2004), so we measured the expression levels of related genes and enzyme activities in the *flo23* mutant. With reduction of Fru-2,6-P_2 content, PFPase enzyme activity was down-regulated and cFBPase activity was slightly elevated in *flo23* mutant (Fig. 6 C and D). The expression of detected related genes all increased/reduced (Fig. S9A, B). All these data indicated that the Arg-379-His is essential for F6P,2-K activity.

AGPase is the rate-limiting enzyme in starch biosynthesis, catalysing the reaction of glucose-1-phosphate (G1P) and ATP to ADP-Glc (Martin and Smith, 1995). ATP content and AGPase activity and PPi content were significantly reduced in developing endosperm of the *flo23* mutant at 9 DAF endosperm, in turn reducing the supply of PPi (Fig. 6E-H). PPi is a replaceable metabolic energy supply, lack of which can lead to inactivation of PPi-dependent energy metabolism processes (Lee and Jeon, 2020). OsPPDKB and pyruvate kinase (OsPK1) are PPi-utilizing enzymes in addition to PFPase; both are key enzymes in the glycolytic pathway and their mutants are also characterized by opaque endosperm (Cai et al., 2018b; Kang et al., 2005). PEP and pyruvate, the most important products of glycolysis, were drastically reduced in the *flo23* mutant (Fig. 6H, I). RT-qPCR revealed that *OsPK1* and *OsPPDKB* were highly expressed in the *flo23* mutant (Fig. S9C) while the protein levels were significantly lower in the developing endosperm (Fig. 6 J). These results indicated that glycolytic steps involving PPi-utilizing enzymes were impaired.

3.7. *Defective glycolysis and storage product accumulation in endosperm of the flo23 mutant*

To understand how *OsF2KP2* affects rice endosperm development in rice, we performed transcriptome sequencing analysis and targeted metabolomic analysis of developing endosperms in the wild type and *flo23* mutant at 9 DAF. A total of 3417 differentially expressed genes (DEGs) were detected; 1421 upregulated and 1996 downregulated (N22 *vs. flo23* , Q value ≤ 0.05 and $|\log_2 FC = \geq 1$) (Fig. 7 A, Table S2). Further analysis showed that the DEGs were annotated to 116 different KEGG pathways. DEGs were mainly enriched in energy metabolism and substance synthesis, especially glycolysis (ko00010), pyruvate metabolism (ko00620), starch and sucrose metabolism (ko00500), lipid metabolism (ko01212) and amino acid metabolism (ko01230) (Fig. 7B). Our heatmap cluster analysis of DEGs involved in glycolysis showed that most genes were down-regulated in the *flo23* mutant, including *fructose-bisphosphate aldolase* (*Os08g0120600*) (Fig. 7 C), but many genes involved in seed development were up-regulated (Fig. S10). Targeted metabolome results showed that the gluconeogenesis and glycolysis pathways were abnormal. The contents of triose phosphates (glyceraldehyde 3-phosphate, 3-phosphoglycerate) were reduced, and conversion of hexose phosphate to triose phosphate was disrupted (Fig. 7D). To identify core gene modules related to *OsF2KP2* from the DEGs, a protein-protein interaction network (PPI) was constructed; 417 high confidence genes were filtered into the PPI network, including 417 nodes and 626 edges (Fig. S11). In order to detect the important modules in the PPI network, the cytohubba plug-in was used to extract the core module,

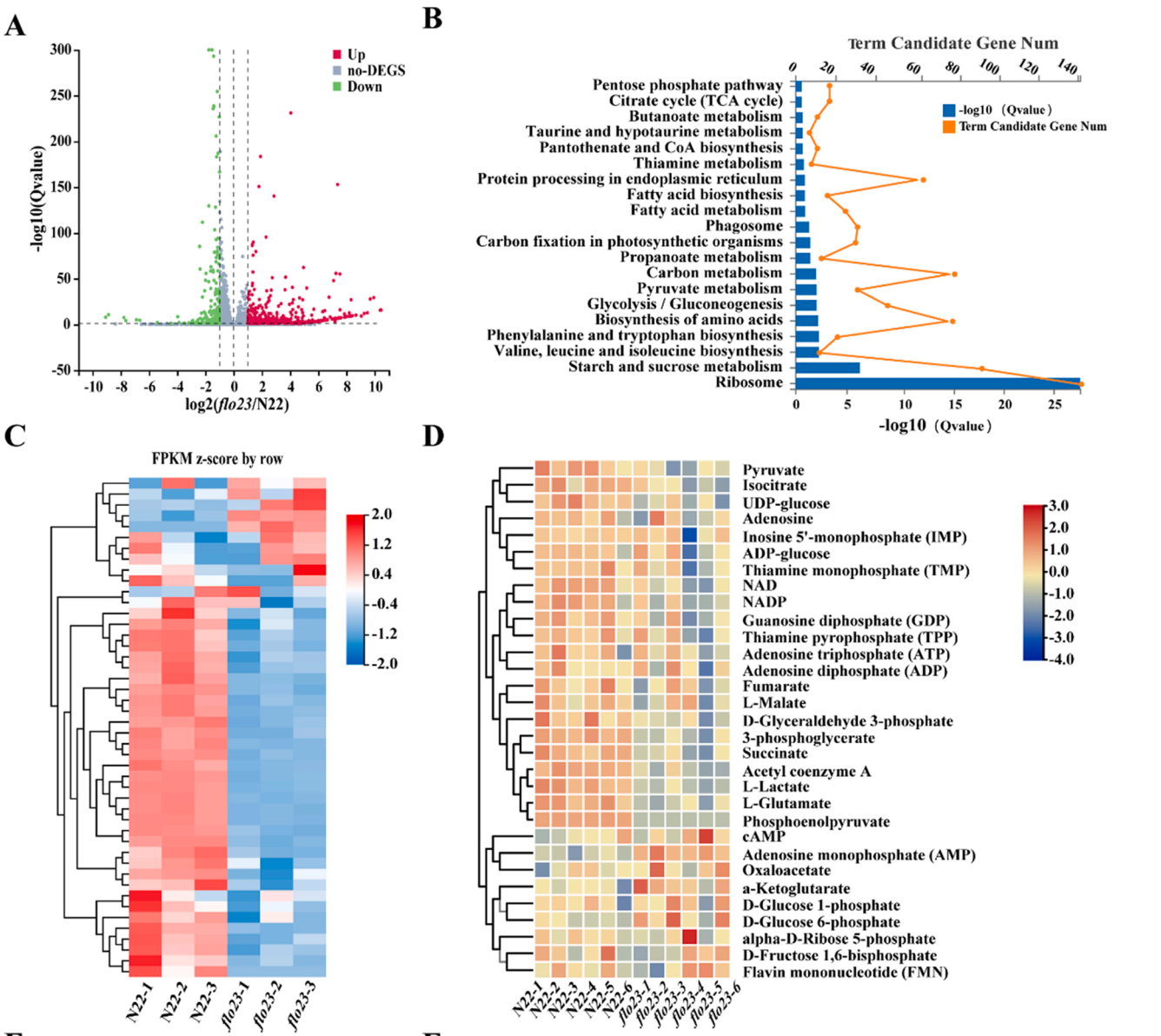

(caption on next page)

Fig. 7. The *OsF2KP2* mutation affects metabolism of storage products and energy in rice endosperm. (A) Volcano plots displaying down-regulated, neutral and up-regulated genes between the wild type and *flo23* mutant in developing endosperm at 9 DAF. (N22 *vs. flo23* , Q value ≤ 0.05 and |log2FC= ≥ 1). (B) Histogram of the top 20 KEGG. The orange polyline reflects the number of genes enriched in each term, and the histogram reflects the Q-value. (C) Hierarchical clustering and heat map of DEGs involved in glycolysis between the wild-type and *flo23* mutant (Q-value ≤ 0.05 and |log2FC= ≥ 1). Color coding represents the range of log2 fold induction (red) or repression (blue). (D) Targeted metabolomic analysis developing endosperm at 9 DAF in the wild type and *flo23*. TBtools was used to visualize the results. (E) PPI networks of genes involved in the starch and sucrose metabolism network up-regulated by *OsF2KP2* and generated by STRING (https://cn.string-db.org/) and constructed by Cytoscape 3.8.2 (https://cytoscape.org/). Node size represents the node degree, and red and yellow nodes indicate hub nodes. (F) KEGG pathway enrichment analysis of the core PPI module indicated that genes with the highest degree of interaction were associated with starch and sucrose metabolism and the energy cycle pathway.

which contained 101 nodes and 235 edges (Fig. 7E). Among the core PPI module, 15 genes with the highest degree of interaction were selected as the hub node; these were involved in starch and sucrose metabolism, TCA cycle, pyruvate metabolism, and glycolysis, consistent with the above results (Fig. 7 F). In conclusion, mutation of *OsF2KP2* disrupted substance and energy metabolism in rice endosperm.

4. Discussion

4.1. Defective amyloplast morphology and starch biosynthesis in the *flo23*mutant

In this study we isolated *flo23* mutant with floury mature endosperm, reduced grain filling rate, and uniformly reduced total starch, amylose, protein, and lipid contents. The *flo23* mutant had abnormal starch granules which only lightly stained with iodine. The amyloplasts had unarranged and fragmented structure. Compared with some other floury mutants, such as *flo6*, *ospk2* and *osnac20/osnac26*, *flo23* mutant show some different phenotypes (Peng et al., 2014; Cai et al., 2018a; Wang et al., 2020b). Firstly, decreased starch biosynthesis in these mutants generally lead to elevated protein and/or lipid contents, while all content of starch, protein and lipid decreased. Secondly, most starch synthesis-related genes in the *flo23* mutant were up-regulated, especially *AGPS2a* and *AGPS2b*. However, the protein levels of both AGPS2a and AGPS2b were slightly decreased, and the reduction of AGPS2a and AGPS2b protein was consistent with the reduction of enzymatic activity assays *in vivo* (Figs. 2D, 6 F). It seems that the up-regulated expression of starch synthesis-related genes was largely due to the feedback regulation. Nevertheless, the underlying effect of the *flo23* mutation might be different from previously reported floury mutants.

Map-based cloning showed that *FLO23* encodes OsF2KP2, a fructose-6-phosphate-2-kinase/fructose-2,6-bisphosphatase (F2KP) with 726 amino acids. OsF2KP2 belongs to a cytoplasm-localized bifunctional enzyme and that the *flo23* mutant had a substitution of Arg by His at amino acid position 379. Arg379 is an active site that is highly conserved in all organisms (Fig. S3) (Furumoto et al., 2001). The enzyme activity experiments *in vitro* and Fru-2,6-P_2 content *in vivo* verified Arg379 is essential for OsF2KP2 enzyme activity. By amino acid alignment, two OsF2KP homologues were identified which share 68 %. However, *OsF2KP2/FLO23* expressed more in developing endosperm, whereas *OsF2KP1* was highly expressed in leaves. The different expression pattern suggests that *OsF2KP1* and *OsF2KP2/FLO23* maybe function in different tissue and developmental stage. And although both *OsF2KP1cr* and *OsF2KP2cr* knock-out mutants showed impaired appearance of grain in rice, but loss function of *OsF2KP2/FLO23* caused much stronger phenotype, floury endosperm. This functional differentiation is quite similar to previous reports on other floury mutants, such as *flo4* and *flo6* (Peng et al., 2014; Kang et al., 2005). In addition, the expression of *OsF2KP1* was elevated in *flo23* mutant (Fig. 5 A). Considering the high sequence similarity of OsF2KP1 and OsF2KP2 and white-core endosperm in *OsF2KP1cr* mutant, OsF2KPs probably have functional redundancy. Notably, F2KPs could interact with each other demonstrated by Y2H, BiFC and Co-IP assays. However, considering the different expression patterns, OsF2KPs are more likely to form self-multimers *in vivo*.

4.2. Mutation in OsF2KP2 leads to multiple disorders in metabolic processes

Previous studies demonstrated that Fru-2,6-P_2 regulates the cytosolic conversion between fructose-1,6-bisphosphate (Fru-1,6-P_2) and fructose-6-phosphate (Fru-6-P) mainly by inhibiting cFBPase and activating PFPase in spinach and wheat leaves (Nielsen et al., 2004; Trevanion, 2002). Disruption of the *cFBPase* gene resulted in a dwarf phenotype and important metabolite changes in both Arabidopsis *atcfbp1* and rice *oscfbp1* mutants (Lee et al., 2008; Rojas-González et al., 2015). Low concentrations of Fru-2,6-P_2 contributed to increased flow of photosynthetic products to sucrose biosynthesis in Arabidopsis leaves (McCormick and Kruger, 2015). In cells of photosynthetic tissue cFBPase and PFPase jointly control the flow of photosynthetic products to glycolysis or starch synthesis (Nielsen et al., 2004). Reduced Fru-2,6-P_2 content in potato tubers caused moderate increase hexoses and a decrease starch synthesis when supplied ^{14}C-labeled sucrose. This finding suggested a compromised sucrose-to-starch transition (Nielsen et al., 2004). In the maize *opaque2* mutant, which is defective in starch biosynthesis, *PFPα* is decreased, but in *o2*-suppressed lines (quality protein maize, QPM) *PFPα* is significantly increased (Guo et al., 2012). In rice PFP1$_\beta$ modulates endosperm metabolism potentially through reversible adjustments to metabolic fluxes (Chen et al., 2020; Duan et al., 2016). Despite these studies, little is known about the effect of Fru-2,6-P_2 on starch synthesis in sink tissues.

In this study, mutation of OsF2KP2 in the *flo23* mutant led to reduced content of Fru-2,6-P_2, which in turn increased FBP activity and decreased PFP (Fig. 6A-C). The change in enzyme activity leading to decreases in glyceraldehyde 3-phosphate and 3-phosphoglycerate probably affected conversion of hexose phosphate to triose phosphate. In addition, reduced triose phosphate and the precursor of amino acid synthesis caused abnormal amino acid metabolism, which was consistent with the KEGG enrichment in the transcriptome (Fig. 7 B, D). The protein levels of OsPK1 and OsPPDKB, the last important enzymes in glycolysis, were clearly lower in developing endosperm of the *flo23* muatant (Fig. 6 J). PEP and pyruvate are converted by OsPKs and OsPPDKs to provide carbon (acetyl-CoA) to the citrate cycle (TCA cycle) in generating ATP, which is required for starch biosynthesis (Cai et al., 2018b; Smith et al., 2000; Andre et al., 2007). The contents of PEP and pyruvate in endosperm of the *flo23* mutant were reduced to one-third of wild type, resulting in compromised fatty acid synthesis (FAS) and TCA cycle (Fig. 6H, I). Decreased AGPase activity might also reduce PPi supply in the *flo23* mutant (Fig. 6F). PFP reversibly converts Fru-6-P and PPi to Fru-1,6-P_2 and OsPPDKB promotes AGPase activity by directly consuming PPi released from the conversion of Glc-1-P to ADP-Glc, enhancing starch metabolism and reducing lipid biosynthesis (Lappe et al., 2018). The activities of PPi-utilizing enzymes OsPK1 and OsPPDKB were further reduced possibly resulting from decreased PPi (Fig. 6G). Finally, the biosynthesis of starch, lipids and amino acids was affected in the *flo23* mutant (Fig. S12). Taken together, Fru-2,6-P_2 reduced the contents of PEP and pyruvate and supply of PPi by changing cFBPase and PFPase, resulting in abnormal biosynthesis of storage products in endosperm cells of the *flo23*mutant.

CRediT authorship contribution statement

Jianmin Wan and **Yihua Wang** designed and conceived the research. **Yihua Wang** provided the *flo23* mutant material. **Xiaoli Chen, Yi Ji, Weiying Zhao, Huanying Niu, Xue Yang, Xiaokang Jiang, Yipeng Zhang** performed the experiments. **Jie Lei, Hang Yang, Rongbo Chen, Chuanwei Gu** and **Hongyi Xu** completed the field work. **Xiaoli Chen** wrote the paper. **Yihua Wang, Yunlong Wang, Erchao Duan, Xuan Teng, Yuanyan Zhang, Wenwei Zhang** and **Hui Dong** revised the paper.

Declaration of Competing Interest

The authors declare that they have no known competing financial interests or personal relationships that could have appeared to influence the work reported in this paper".

Data availability

Data will be made available on request.

Acknowledgements

This work was supported by grants from the "JBGS" Project of Seed Industry Revitalization in Jiangsu Province (JBGS[2021]008), Jiangsu Province Agriculture Independent Innovation Fund Project (CX(19) 1002), the Key R&D Program of Jiangsu Province (BE2021359), This work was also supported by the Key Laboratory of Biology, Genetics, and Breeding of Japonica Rice in Mid-lower Yangtze River, Ministry of Agriculture, P.R. China, the Jiangsu Collaborative innovation Center for Modern Crop Production, and Jiangsu Nanjing National Field Scientific Observation and Research Station for Rice Germplasm Resources.

Appendix A. Supporting information

Supplementary data associated with this article can be found in the online version at doi:10.1016/j.plantsci.2022.111503.

References

C. Andre, J.E. Froehlich, M.R. Moll, C. Benning, A heteromeric plastidic pyruvate kinase complex involved in seed oil biosynthesis in Arabidopsis, Plant Cell 19 (2007) 2006–2022.

Y. Cai, S. Li, G. Jiao, Z. Sheng, Y. Wu, G. Shao, L. Xie, C. Peng, J. Xu, S. Tang, X. Wei, P. Hu, *OsPK2* encodes a plastidic pyruvate kinase involved in rice endosperm starch synthesis, compound granule formation and grain filling, Plant Biotechnol. J. 16 (2018a) 1878–1891.

Y. Cai, W. Zhang, J. Jin, X. Yang, X. You, H. Yan, L. Wang, J. Chen, J. Xu, W. Chen, X. Chen, J. Ma, X. Tang, F. Kong, X. Zhu, G. Wang, L. Jiang, W. Terzaghi, C. Wang, J. Wan, *OsPKpα1* encodes a plastidic pyruvate kinase that affects starch biosynthesis in the rice endosperm, J. Integr. Plant Biol. 60 (2018b) 1097–1118.

C. Chen, B. He, X. Liu, X. Ma, Y. Liu, H.Y. Yao, P. Zhang, J. Yin, X. Wei, H.J. Koh, C. Yang, H.W. Xue, Z. Fang, Y. Qiao, Pyrophosphate-fructose 6-phosphate 1-phosphotransferase (PFP1) regulates starch biosynthesis and seed development via heterotetramer formation in rice (*Oryza sativa* L.), Plant Biotechnol. J. 18 (2020) 83–95.

S. Chen, L. Tao, L. Zeng, M.E. Vega-Sanchez, K. Umemura, G.L. Wang, A highly efficient transient protoplast system for analyzing defence gene expression and protein-protein interactions in rice, Mol. Plant Pathol. 7 (2006) 417–427.

H. Draborg, D. Villadsen, T.H. Nielsen, Transgenic Arabidopsis plants with decreased activity of fructose-6-phosphate,2-kinase/fructose-2,6-bisphosphatase have altered carbon partitioning, Plant Physiol. 126 (2001) 750–758.

E. Duan, Y. Wang, L. Liu, J. Zhu, M. Zhong, H. Zhang, S. Li, B. Ding, X. Zhang, X. Guo, L. Jiang, J. Wan, Pyrophosphate: fructose-6-phosphate 1-phosphotransferase (PFP) regulates carbon metabolism during grain filling in rice, Plant Cell Rep. 35 (2016) 1321–1331.

N. Fujita, R. Satoh, A. Hayashi, M. Kodama, R. Itoh, S. Aihara, Y. Nakamura, Starch biosynthesis in rice endosperm requires the presence of either starch synthase I or IIIa, J. Exp. Bot. 62 (2011) 4819–4831.

T. Furumoto, M. Teramoto, N. Inada, M. Ito, I. Nishida, A. Watanabe, Phosphorylation of a bifunctional enzyme, 6-phosphofructo-2-kinase/fructose-2,6-bisphosphate 2-phosphatase, is regulated physiologically and developmentally in rosette leaves of *Arabidopsis thaliana*, Plant Cell Physiol. 42 (2001) 1044–1048.

X. Guo, K. Ronhovde, L. Yuan, B. Yao, M.P. Soundararajan, T. Elthon, C. Zhang, D. R. Holding, Pyrophosphate-dependent fructose-6-phosphate 1-phosphotransferase induction and attenuation of Hsp gene expression during endosperm modification in quality protein maize, Plant Physiol. 158 (2012) 917–929.

X. Han, Y. Wang, X. Liu, L. Jiang, Y. Ren, F. Liu, C. Peng, J. Li, X. Jin, F. Wu, J. Wang, X. Guo, X. Zhang, Z. Cheng, J. Wan, The failure to express a protein disulphide isomerase-like protein results in a floury endosperm and an endoplasmic reticulum stress response in rice, J. Exp. Bot. 63 (2012) 121–130.

Y. Hao, Y. Wang, M. Wu, X. Zhu, X. Teng, Y. Sun, J. Zhu, Y. Zhang, R. Jing, J. Lei, J. Li, X. Bao, C. Wang, Y. Wang, J. Wan, The nuclear-localized PPR protein OsNPPR1 is important for mitochondrial function and endosperm development in rice, J. Exp. Bot. 70 (2019) 4705–4720.

R.E. Häusler, K.L. Fischer, U.I. Flügge, Determination of low-abundant metabolites in plant extracts by NAD(P)H fluorescence with a microtiter plate reader, Anal. Biochem 281 (2000) 1–8.

L. Hu, B. Tu, W. Yang, H. Yuan, J. Li, L. Guo, L. Zheng, W. Chen, X. Zhu, Y. Wang, P. Qin, B. Ma, S. Li, Mitochondria-associated pyruvate kinase complexes regulate grain filling in rice, Plant Physiol. 183 (2020) 1073–1087.

T. Hu, Y. Tian, J. Zhu, Y. Wang, R. Jing, J. Lei, Y. Sun, Y. Yu, J. Li, X. Chen, X. Zhu, Y. Hao, L. Liu, Y. Wang, J. Wan, *OsNDUFA9* encoding a mitochondrial complex I subunit is essential for embryo development and starch synthesis in rice, Plant Cell Rep. 37 (2018) 1667–1679.

H.G. Kang, S. Park, M. Matsuoka, G. An, White-core endosperm floury endosperm-4 in rice is generated by knockout mutations in the C-type pyruvate orthophosphate dikinase gene (*OsPPDKB*), Plant J. 42 (2005) 901–911.

Y. Kawagoe, A. Kubo, H. Satoh, F. Takaiwa, Y. Nakamura, Roles of isoamylase and ADP-glucose pyrophosphorylase in starch granule synthesis in rice endosperm, Plant J. 42 (2005) 164–174.

R.R. Lappe, J.W. Baier, S.K. Boehlein, R. Huffman, Q. Lin, F. Wattebled, A.M. Settles, L. C. Hannah, L. Borisjuk, H. Rolletschek, J.D. Stewart, M.P. Scott, T.A. Hennen-Bierwagen, A.M. Myers, Functions of maize genes encoding pyruvate phosphate dikinase in developing endosperm, Proc. Natl. Acad. Sci. USA 115 (2018) E24-e33.

S.K. Lee, J.S. Jeon, Review: crucial role of inorganic pyrophosphate in integrating carbon metabolism from sucrose breakdown to starch synthesis in rice endosperm, Plant Sci. 298 (2020), 110572.

S.K. Lee, J.S. Jeon, F. Börnke, L. Voll, J.I. Cho, C.H. Goh, S.W. Jeong, Y.I. Park, S.J. Kim, S.B. Choi, A. Miyao, H. Hirochika, G. An, M.H. Cho, S.H. Bhoo, U. Sonnewald, T. R. Hahn, Loss of cytosolic fructose-1,6-bisphosphatase limits photosynthetic sucrose synthesis and causes severe growth retardations in rice (*Oryza sativa*), Plant Cell Environ. 31 (2008) 1851–1863.

Y.H. Lee, D.S. Lee, J.M. Lim, J.M. Yoon, S.H. Bhoo, J.S. Jeon, T.R. Hahn, Carbon-partitioning in Arabidopsis is regulated by the Fructose 6-phosphate, 2-Kinase/Fructose 2,6-bisphosphatase enzyme, J. Plant Biol. 49 (2006) 70–79.

J. Lei, X. Teng, Y. Wang, X. Jiang, H. Zhao, X. Zheng, Y. Ren, H. Dong, Y. Wang, E. Duan, Y. Zhang, W. Zhang, H. Yang, X. Chen, R. Chen, Y. Zhang, M. Yu, S. Xu, X. Bao, P. Zhang, S. Liu, X. Liu, Y. Tian, L. Jiang, Y. Wang, J. Wan, Plastidic pyruvate dehydrogenase complex E1 component subunit Alpha1 is involved in galactolipid biosynthesis required for amyloplast development in rice, Plant Biotechnol. J. 20 (2022) 437–453.

W. Long, Y. Wang, S. Zhu, W. Jing, Y. Wang, Y. Ren, Y. Tian, S. Liu, X. Liu, L. Chen, D. Wang, M. Zhong, Y. Zhang, T. Hu, J. Zhu, Y. Hao, X. Zhu, W. Zhang, C. Wang, W. Zhang, J. Wan, *FLOURY SHRUNKEN ENDOSPERM1* connects phospholipid metabolism and amyloplast development in rice, Plant Physiol. 177 (2018) 698–712.

J.E. Markham, N.J. Kruger, Kinetic properties of bifunctional 6-phosphofructo-2-kinase/fructose-2,6-bisphosphatase from spinach leaves, Eur. J. Biochem. 269 (2002) 1267–1277.

C. Martin, A.M. Smith, Starch biosynthesis, Plant Cell 7 (1995) 971–985.

A.J. McCormick, N.J. Kruger, Lack of fructose 2,6-bisphosphate compromises photosynthesis and growth in Arabidopsis in fluctuating environments, Plant J. 81 (2015) 670–683.

T.H. Nielsen, J.H. Rung, D. Villadsen, Fructose-2,6-bisphosphate: a traffic signal in plant metabolism, Trends Plant Sci. 9 (2004) 556–563.

T.H. Nielsen, M. Stitt, Tobacco transformants with strongly decreased expression of *pyrophosphate:fructose-6-phosphate* expression in the base of their young growing leaves contain much higher levels of fructose-2,6-bisphosphate but no major changes in fluxes, Planta 214 (2001) 106–116.

M. Ohashi, K. Ishiyama, M. Kusano, A. Fukushima, S. Kojima, T. Hayakawa, T. Yamaya, Reduction in sucrose contents by downregulation of fructose-1,6-bisphosphatase 2 causes tiller outgrowth cessation in rice mutants lacking *glutamine synthetase1;2*, Rice 11 (2018) 65.

S. Park, M.H. Cho, S.H. Bhoo, J.S. Jeon, Y.K. Kwon, T.R. Hahn, Altered sucrose synthesis in rice plants with reduced activity of fructose-6-phosphate 2-kinase/fructose-2,6-bisphosphatase, J. Plant Biol. 50 (2007) 38.

C. Peng, Y. Wang, F. Liu, Y. Ren, K. Zhou, J. Lv, M. Zheng, S. Zhao, L. Zhang, C. Wang, L. Jiang, X. Zhang, X. Guo, Y. Bao, J. Wan, *FLOURY ENDOSPERM6* encodes a CBM48 domain-containing protein involved in compound granule formation and starch synthesis in rice endosperm, Plant J. 77 (2014) 917–930.

J.A. Rojas-González, M. Soto-Súarez, Á. García-Díaz, M.C. Romero-Puertas, L. M. Sandalio, Á. Mérida, I. Thormählen, P. Geigenberger, A.J. Serrato, M. Sahrawy, Disruption of both chloroplastic and cytosolic FBPase genes results in a dwarf phenotype and important starch and metabolite changes in *Arabidopsis thaliana*, J. Exp. Bot. 66 (2015) 2673–2689.

J.H. Rung, H.H. Draborg, K. Jørgensen, T.H. Nielsen, Carbon partitioning in leaves and tubers of transgenic potato plants with reduced activity of fructose-6-phosphate,2-kinase/fructose-2,6-bisphosphatase, Physiol. Plant 121 (2004) 204–214.

N. Ryoo, C. Yu, C.S. Park, M.Y. Baik, I.M. Park, M.H. Cho, S.H. Bhoo, G. An, T.R. Hahn, J. S. Jeon, Knockout of a starch synthase gene *OsSSIIIa/Flo5* causes white-core floury endosperm in rice (*Oryza sativa* L.), Plant Cell Rep. 26 (2007) 1083–1095.

H. Satoh, A. Nishi, K. Yamashita, Y. Takemoto, Y. Tanaka, Y. Hosaka, A. Sakurai, N. Fujita, Y. Nakamura, Starch-branching enzyme I-deficient mutation specifically affects the structure and properties of starch in rice endosperm, Plant Physiol. 133 (2003) 1111–1121.

P. Scott, A.J. Lange, N.J. Kruger, Photosynthetic carbon metabolism in leaves of transgenic tobacco (*Nicotiana tabacum* L.) containing decreased amounts of fructose 2,6-bisphosphate, Planta 211 (2000) 864–873.

K.C. She, H. Kusano, K. Koizumi, H. Yamakawa, M. Hakata, T. Imamura, M. Fukuda, N. Naito, Y. Tsurumaki, M. Yaeshima, T. Tsuge, K. Matsumoto, M. Kudoh, E. Itoh, S. Kikuchi, N. Kishimoto, J. Yazaki, T. Ando, M. Yano, T. Aoyama, T. Sasaki, H. Satoh, H. Shimada, A novel factor *FLOURY ENDOSPERM2* is involved in regulation of rice grain size and starch quality, Plant Cell 22 (2010) 3280–3294.

C.R. Smith, V.L. Knowles, W.C. Plaxton, Purification and characterization of cytosolic pyruvate kinase from *Brassica napus* (rapeseed) suspension cell cultures: implications for the integration of glycolysis with nitrogen assimilation, Eur. J. Biochem. 267 (2000) 4477–4485.

M. Stitt, Fructose-2,6-Bisphosphate as a regulatory molecule in plants, Annu Rev. Plant Biol. 41 (1990a) 153–185.

M. Stitt, Fructose-2,6-Bisphosphate as a regulatory molecule in plants, Annu Rev. Plant Biol. 41 (1990b) 153–185.

R. Suzuki, T. Imamura, Y. Nonaga, H. Kusano, H. Teramura, K.T. Sekine, T. Yamashita, H. Shimada, A novel FLOURY ENDOSPERM2 (FLO2)-interacting protein, is involved in maintaining fertility and seed quality in rice, Plant Biotechnol. 37 (2020) 47–55.

A. Szoke, E. Kiss, L. Heszky, I. Kerepesi, O. Toldi, Effects of altered Fructose 2,6-Bisphosphate levels on carbohydrate metabolism in carnation, Hortscience 42 (2007) 403–406.

R. Tabassum, T. Dosaka, H. Ichida, R. Morita, Y. Ding, T. Abe, T. Katsube-Tanaka, *FLOURY ENDOSPERM11-2* encodes plastid HSP70-2 involved with the temperature-dependent chalkiness of rice (*Oryza sativa* L.) grains, Plant J. 103 (2020) 604–616.

X.J. Tang, C. Peng, J. Zhang, Y. Cai, X.M. You, F. Kong, H.G. Yan, G.X. Wang, L. Wang, J. Jin, W.W. Chen, X.G. Chen, J. Ma, P. Wang, L. Jiang, W.W. Zhang, J.M. Wan, ADP-glucose pyrophosphorylase large subunit 2 is essential for storage substance accumulation and subunit interactions in rice endosperm, Plant Sci. 249 (2016) 70–83.

X. Teng, M. Zhong, X. Zhu, C. Wang, Y. Ren, Y. Wang, H. Zhang, L. Jiang, D. Wang, Y. Hao, M. Wu, J. Zhu, X. Zhang, X. Guo, Y. Wang, J. Wan, *FLOURY ENDOSPERM16* encoding a NAD-dependent cytosolic malate dehydrogenase plays an important role in starch synthesis and seed development in rice, Plant Biotechnol. J. 17 (2019) 1914–1927.

Y. Toyosawa, Y. Kawagoe, R. Matsushima, N. Crofts, M. Ogawa, M. Fukuda, T. Kumamaru, Y. Okazaki, M. Kusano, K. Saito, K. Toyooka, M. Sato, Y. Ai, J.L. Jane, Y. Nakamura, N. Fujita, Deficiency of Starch Synthase IIIa and IVb alters starch granule morphology from polyhedral to spherical in rice endosperm, Plant Physiol. 170 (2016) 1255–1270.

S.J. Trevanion, Regulation of sucrose and starch synthesis in wheat (*Triticum aestivum* L.) leaves: role of fructose 2,6-bisphosphate, Planta 215 (2002) 653–665.

M.J. van der Merwe, J.H. Groenewald, M. Stitt, J. Kossmann, F.C. Botha, Downregulation of pyrophosphate: D-fructose-6-phosphate 1-phosphotransferase activity in sugarcane culms enhances sucrose accumulation due to elevated hexose-phosphate levels, Planta 231 (2010) 595–608.

H. Wang, T.H. Ham, D.E. Im, S.M. Lar, S.G. Jang, J. Lee, Y. Mo, J.U. Jeung, S.T. Kim, S. W. Kwon, A new SNP in rice gene encoding pyruvate phosphate dikinase (PPDK) associated with floury endosperm, Genes 11 (2020a).

H. Wang, Y.J. Mo, D.E. Im, S.G. Jang, T.H. Ham, J. Lee, J.U. Jeung, S.W. Kwon, A new SNP in *cyOsPPDK* gene is associated with floury endosperm in Suweon 542, Mol. Genet. Genom. 293 (2018) 1151–1158.

J. Wang, Z. Chen, Q. Zhang, S. Meng, C. Wei, The NAC transcription factors *OsNAC20* and *OsNAC26* regulate starch and storage protein synthesis, Plant Physiol. 184 (2020b) 1775–1791.

Y. Wang, Y. Ren, X. Liu, L. Jiang, L. Chen, X. Han, M. Jin, S. Liu, F. Liu, J. Lv, K. Zhou, N. Su, Y. Bao, J. Wan, OsRab5a regulates endomembrane organization and storage protein trafficking in rice endosperm cells, Plant J. 64 (2010) 812–824.

M. Wu, Y. Ren, M. Cai, Y. Wang, S. Zhu, J. Zhu, Y. Hao, X. Teng, X. Zhu, R. Jing, H. Zhang, M. Zhong, Y. Wang, C. Lei, X. Zhang, X. Guo, Z. Cheng, Q. Lin, J. Wang, L. Jiang, Y. Bao, Y. Wang, J. Wan, Rice *FLOURY ENDOSPERM10* encodes a pentatricopeptide repeat protein that is essential for the trans-splicing of mitochondrial *nad1* intron 1 and endosperm development, New Phytol. 223 (2019) 736–750.

X. You, W. Zhang, J. Hu, R. Jing, Y. Cai, Z. Feng, F. Kong, J. Zhang, H. Yan, W. Chen, X. Chen, J. Ma, X. Tang, P. Wang, S. Zhu, L. Liu, L. Jiang, J. Wan, *FLOURY ENDOSPERM15* encodes a glyoxalase I involved in compound granule formation and starch synthesis in rice endosperm, Plant Cell Rep. 38 (2019) 345–359.

M. Yu, M. Wu, Y. Ren, Y. Wang, J. Li, C. Lei, Y. Sun, X. Bao, H. Wu, H. Yang, T. Pan, Y. Wang, R. Jing, M. Yan, H. Zhang, L. Zhao, Z. Zhao, X. Zhang, X. Guo, Z. Cheng, B. Yang, L. Jiang, J. Wan, Rice *FLOURY ENDOSPERM 18* encodes a pentatricopeptide repeat protein required for 5′ processing of mitochondrial *nad5* messenger RNA and endosperm development, J. Integr. Plant Biol. 63 (2021) 834–847.

Y. Zhang, W. Xiao, L. Luo, J. Pang, W. Rong, C. He, Downregulation of *OsPK1*, a cytosolic pyruvate kinase, by T-DNA insertion causes dwarfism and panicle enclosure in rice, Planta 235 (2012) 25–38.

M. Zhong, X. Liu, F. Liu, Y. Ren, Y. Wang, J. Zhu, X. Teng, E. Duan, F. Wang, H. Zhang, M. Wu, Y. Hao, X. Zhu, R. Jing, X. Guo, L. Jiang, Y. Wang, J. Wan, *FLOURY ENDOSPERM12* encoding Alanine aminotransferase 1 regulates carbon and nitrogen metabolism in rice, J. Plant Biol. 62 (2019) 61–73.

H. Zhou, L. Wang, G. Liu, X. Meng, Y. Jing, X. Shu, X. Kong, J. Sun, H. Yu, S.M. Smith, D. Wu, J. Li, Critical roles of soluble starch synthase *SSIIIa* and granule-bound starch synthase *Waxy* in synthesizing resistant starch in rice, Proc. Natl. Acad. Sci. USA 113 (2016) 12844–12849.

X. Zhu, X. Teng, Y. Wang, Y. Hao, R. Jing, Y. Wang, Y. Liu, J. Zhu, M. Wu, M. Zhong, X. Chen, Y. Zhang, W. Zhang, C. Wang, Y. Wang, J. Wan, *FLOURY ENDOSPERM11* encoding a plastid heat shock protein 70 is essential for amyloplast development in rice, Plant Sci. 277 (2018) 89–99.